iScience

CellPress
OPEN ACCESS

Article

Development of an adipose-tropic AAV capsid ablating liver tropism

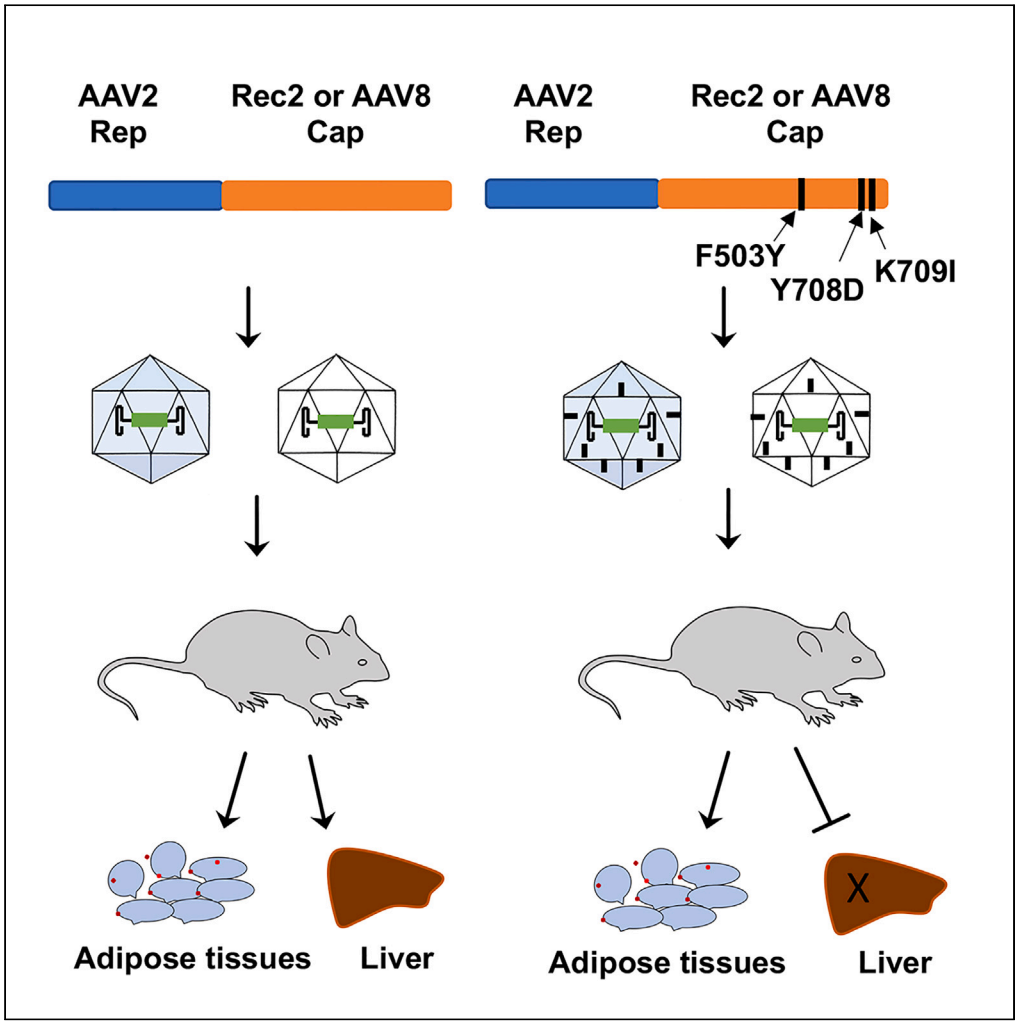

Wei Huang, Rhiannon Bates, Bhavya Appana, Tawfiq Mohammed, Lei Cao

lei.cao@osumc.edu

Highlights

AAV vectors targeting adipose tissue are underdeveloped

F503Y/Y708D/K709I substitution in AAV8 and Rec2 capsids ablates liver tropism

Rec2 variant V7 with F503Y/Y708D/K709I substitution is highly adipo-tropic

V7 vector-based gene therapy rescues metabolic defects of *ob/ob* mice at a low dose

Huang et al., iScience *27*, 110930
October 18, 2024
https://doi.org/10.1016/j.isci.2024.110930

iScience

CellPress
OPEN ACCESS

Article

Development of an adipose-tropic AAV capsid ablating liver tropism

Wei Huang,[1,2] Rhiannon Bates,[1,2] Bhavya Appana,[1,2] Tawfiq Mohammed,[1,2] and Lei Cao[1,2,3,*]

SUMMARY

AAV vectors are mainstream delivery platforms in gene therapy, yet AAV-mediated gene transfer to adipose tissue is underdeveloped due to low efficiency of natural AAVs. We previously demonstrated that an engineered capsid Rec2 displayed improved adipo-tropism but with the caveat of liver transduction. To generate highly adipo-tropic capsid, we modified Rec2 capsid by site-specific mutagenesis and found the variant V7 with F503Y, Y708D and K709I substitution to harbor highly selective adipo-tropism while diminishing liver transduction. Intraperitoneal injection favored transduction to visceral fat while intravenous administration favored subcutaneous fat. Intraperitoneal administration of V7 vector harboring human leptin and adiponectin as single transcript normalized the metabolic dysfunction of *ob/ob* mice at a low dose. Moreover, introducing the same mutagenesis to AAV8 capsid diminished liver transduction suggesting F503, Y708 and K709 critical for liver transduction. The Rec2.V7 vector may provide a powerful tool for basic research and potent vehicle for adipose-targeting gene therapy.

INTRODUCTION

Adeno-associated virus (AAV) is a single-stranded DNA virus with non-enveloped capsid. Recombinant AAV vectors are replication defective AAV particles serving as an invaluable tool for genetic manipulation of specific tissues and have been used safely in clinical trials. AAV has become the most popular delivery system for gene therapy due to their non-pathogenic and broad tropism being used in more than 200 ongoing clinical trials.[1,2] AAV vectors have been successful in delivering transgenes to liver, heart, skeletal muscle, brain, and eye.[3] In contrast, adipose tissue, one of the largest organs in the body, playing a pivotal role in physiology and pathologies of multiple diseases, is under-investigated in the field of AAV gene therapy largely due to the low transduction efficiency in adipose tissue of natural AAV serotypes.[4] A comprehensive literature review finds AAV8 the most efficient capsid to transduce adipose tissue among natural AAV serotypes that have been evaluated.[4] However, AAV8 transduces liver far more efficiently than adipose tissue, necessitating methods to restrict off-target transgene expression in the liver.

It is known that modulating AAV capsids affects the viral tissue tropism and the functional role of a provided transgene.[1,5] To specifically manipulate the adipose tissue, we developed an rAAV vector to achieve highly efficient transduction of adipose tissue. The engineered hybrid capsid Rec2, generated by capsid shuffling of AAV8 and rhesus 20 (rh20),[6] can transduce white adipose tissue (WAT) and brown adipose tissue (BAT) far more efficiently than the natural (AAV1, 8, and 9) and engineered capsids (Rec1, Rec3, Rec4) being compared via direct fat pad injection.[7] One limitation is the transduction of liver when the Rec2 vector is injected systemically.[8] To prevent transgene expression in the liver, we engineered the AAV vector genome to contain two expression cassettes: one uses ubiquitous hybrid cytomegalovirus enhancer/chicken β-actin (CBA) promoter to drive the transgene, and the other uses the liver-specific albumin promoter to drive a specific microRNA targeting woodchuck posttranscriptional regulatory element (WPRE) sequence which only exists in the transgene expression cassette. The efficacy of this adipose-specific (AS) dual-cassettes design (named AS/Rec2) was demonstrated in several publications by our lab[9–13] and independently validated by others.[14]

Although there has been a significant advancement in AAV technology targeting the adipose tissue, the AS/Rec2 system has drawbacks: (1) Rec2 vectors are present in the liver and therefore bearing the risk of viral vector-associated toxicity at extremely high dose[15,16]; (2) the dual-cassette design is unable to restrict transgene expression in the liver if the transgenes are miRNA and shRNA; (3) the introduction of the second cassette further exacerbates the size limitation of a transgene (<1750 bp in the current dual-cassette design) and thereby excluding its use for many genes and CRISPR/Cas9 genome editing; (4) restriction of liver transgene expression is less efficient in conditions where the albumin promoter is weakened. For example, we found that AS/Rec2-Fgf21 led to 4.5-fold increase of transgene Fgf21 expression in the liver in 24-month-old mice.[17] In contrast, the same AS/Rec2-Fgf21 vector did not alter Fgf21 expression in the liver of young mice.[12] As such, a capsid with improved adipose tropism and truly diminishing liver tropism is highly desirable.

[1]Department of Cancer Biology & Genetics, College of Medicine, The Ohio State University, Columbus, OH 43210, USA
[2]The Ohio State University Comprehensive Cancer Center, Columbus, OH 43210, USA
[3]Lead contact
*Correspondence: lei.cao@osumc.edu
https://doi.org/10.1016/j.isci.2024.110930

To overcome the limitations of the AS/Rec2 system, we used Rec2 as a template for capsid engineering to generate truly adipose-tropic AAVs while ablating liver tropism. AAV capsid mediates cellular entry and post entry processing (intracellular trafficking), that can dictate the tropism of the vector and level of transgene expression.[18] Capsid modification in many serotypes have been reported to achieve tropism alteration.[1] In this study, we modified Rec2 capsid by site-specific mutagenesis and generated 8 variants of Rec2 capsid. *In vivo* screening found the Rec2 capsid variant with F503Y, Y708D and K709I substitution (referred to Rec2.V7, V7 in short) led to substantial transduction of adipose tissue while no transgene expression was detected in the liver. We further characterized the V7 capsid via different routes of administration and doses and conducted a proof-of-concept study in the congenital leptin deficiency model *ob/ob* mice.

RESULTS

Rec2 capsid modification results in adipo-tropic V7 vector while ablating liver tropism

To search for adipo-tropic vector while ablating liver tropism, we generated 8 variants by mutagenesis in Rec2 capsid sequence (Table S1), named V1∼8. V3 failed to package and discarded. For *in vivo* screening, pseudo-AAV vectors: cis plasmid with AAV2 ITRs and a single cassette to express enhanced green fluorescent protein (referred to GFP), were packaged to native Rec2, and Rec2 capsid variants using the same methods of triple transfection and purification. To screen the variants, we used tissue lysate for direct GFP fluorescence count readout at a 485-nm excitation wavelength with cut-off 528-nm emission wavelength. Adipose tissue is distributed in various location, including visceral or intraperitoneal and subcutaneous fat depots. Commonly referred visceral fat depots in rodent include epididymal (male) or gonadal (female) white adipose tissue (eWAT or gWAT), mesentery white adipose tissue (mWAT), and retroperitoneal white adipose tissue (rWAT). Subcutaneous fat depots include inguinal white adipose tissue (iWAT) and intrascapular brown adipose tissue (BAT).

Intraperitoneal (i.p.) delivery

Upon initial *in vivo* screening at the dose of 2E10 viral genome (vg)/mouse via i.p. injection, V7 capsid vector (Figure 1) led to substantial GFP expression in the eWAT while no GFP fluorescence was detected in the liver (Figure S1). Other variants or vectors at the same dose either failed to alter liver tropism or lost adipose transduction. As such, we selected V7 capsid for further characterization. Mutations in V7 are indicated in Figure 1A and highlighted in its capsid amino acid sequence in Figure 1B.

Next, we repeated i.p. experiment at the dose of 2E10 vg/mouse and verified that GFP fluorescence was detected in eWAT but not in liver in mice receiving V7 vector (Figure 2A). In contrast, GFP fluorescence was detected in both eWAT and liver from mice receiving parent Rec2 vector at same dose. Consistent with GFP fluorescence reading, Western blotting also confirmed V7 vector-mediated transgene expression in adipose tissue, but not liver, while Rec2 resulted in transgene expression in both WAT and liver (Figure 2B). Because V7 vector resulted in lower GFP expression in WAT compared to that of native Rec2 at the dose of 2E10 vg/mouse (Figures 2A and 2B), we conducted a dosing experiment to validate the adipo-tropism of V7 and to estimate the adipose transduction efficiency. Increasing the dose of V7 vector to 4E10 vg/mouse improved transgene expression in eWAT, reaching approximately 40% of native Rec2 at 2E10 vg/mouse (Figure 2C). Of note, i.p. injection of V7 vector led to similar GFP expression in the mesenteric WAT (mWAT) compared to native Rec2. Importantly, V7 vector via i.p. injection displayed specific WAT transgene expression with no GFP fluorescence detected in liver, pancreas, heart, skeletal muscle, spleen, and kidney even at higher dose of 8E10 vg/mouse (Figure 2C). In contrast, Rec2 vector led to strong GFP expression in both WAT and liver, and noticeable amount of GFP in pancreas (Figure 2C). The adipo-tropism of V7 vector was confirmed by a different investigator who packaged the V7 vector and repeated the high dose experiment (Figure 2D). Next, we quantified the viral vector genome copy numbers in eWAT, liver, and other peripheral tissues from mice receiving i.p. injection of V7 vector at high dose (8E10 vg/mouse). V7 vector genome was mostly detected in eWAT (56791 $\pm$ 1302 copy number/50 ng genomic DNA) and barely found in liver (629 $\pm$ 8 copy number/50 ng genomic DNA) (Figure 2E).

Intravenous (i.v.) administration

Next, we examined the biodistribution of V7 vector by i.v. administration. AAV8 is reported to be the most efficient natural serotype for liver-directed gene transfer.[19] We used AAV8 as a positive control in this experiment. Two doses (low dose of 4E10, high dose of 8E10 vg/mouse) were administered via tail vein injection. Western blotting showed V7 vector transduced inguinal WAT (iWAT) and BAT at both low dose and high dose. AAV8 at high dose resulted in GFP protein level in iWAT and BAT comparable to the levels of V7 at low dose (Figure 3A). As expected, AAV8 yielded robust GFP expression in liver with high dose (Figure 3A). In contrast, no liver transgene expression was detected in mice receiving V7 vector even at high dose (Figure 3A). Interestingly, both V7 and AAV8 vector did not yield GFP expression in eWAT. Next, we further examined V7 biodistribution in additional tissues from a mouse receiving high dose V7 vector by Western blotting. GFP expression was detected in fat depots (iWAT, BAT and rWAT) but not in liver, spleen, pancreas, lung, intestine, heart, and kidney (Figure 3B). To further confirm diminished liver tropism of V7 vector, we isolated total RNA from iWAT and liver, and quantified transgene GFP mRNA levels by qRT-PCR. Saline injection served as negative control. Cycle threshold (Ct) values of GFP from mice receiving V7 and AAV8 vectors were subtracted from saline control. β-actin was house-keeping gene for qRT-PCR. As shown in Table S2, GFP mRNA expression was detected in iWAT but not liver in mice receiving V7. In contrast, GFP mRNA was detected in both liver and iWAT for AAV8. In addition, we measured vector genome copy numbers in iWAT and liver of mice receiving i.v. injection of either V7 or AAV8 vector at high dose (8E10 vg/mouse). V7 vector genome was mostly detected in iWAT (127216 $\pm$ 14778 genome copy number/50 ng genomic DNA) and was found barely in liver (1034 $\pm$ 16 genome copy number/50 ng genomic DNA) (Figure 3C). Consistent with protein and mRNA data, the vast majority AAV8 vector was accumulated in liver (199099 $\pm$ 3877 genome copy number/50 ng genomic DNA) vs. in iWAT (25111 $\pm$ 3332 genome copy number/50 ng genomic DNA) (Figure 3C).

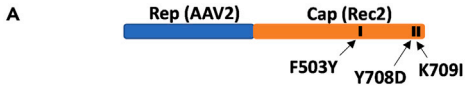

B V7 capsid amino acid sequence

```
MAADGYLPDWLEDNLSEGIREWWDLKPGAPKPKANQQKQDDGRGLVLPGY 50
KYLGPFNGLDKGEPVNAADAAALEHDKAYDQQLKAGDNPYLRYNHADAEF 100
QERLQEDTSFGGNLGRAVFQAKKRVLEPLGLVEEGAKTAPGKKRPVEPSP 150
QRSPDSSTGIGKTGQQPAKKRLNFGQTGDSESVPDPQPIGEPPAGPSGLG 200
SGTMAAGGGAPMADNNEGADGVGSSSGNWHCDSTWLGDRVITTSTRTWAL 250
PTYNNHLYKQISNGTSGGSTNDNTYFGYSTPWGYFDFNRFHCHFSPRDWQ 300
RLINNNWGFRPKRLNFKLFNIQVKEVTQNEGTKTIANNLTSTIQVFTDSE 350
YQLPYVLGSAHQGCLPPFPADVFMIPQYGYLTLNNGSQAVGRSSFYCLEY 400
FPSQMLRTGNNFEFSYQFEDVPFHSSYAHSQSLDRLMNPLIDQYLYYLSR 450
TQSTGGTAGTQQLLFSQAGPNNMSAQAKNWLPGPCYRQQRVSTTTGQNNN 500
SNYAWTAGTKYHLNGRNSLANPGIAMATHKDDEERFFPSNGILIFGKQNA 550
ARDNADYSDVMLTSEEEIKTTNPVATEEYGIVADNLQQQNTAPQIGTVNS 600
QGALPGMVWQNRDVYLQGPIWAKIPHTDGNFHPSPLMGGFGLKHPPPQIL 650
IKNTPVPADPPTTFNQSKLNSFITQYSTGQVSVEIEWELQKENSKRWNPE 700
IQYTSNYDISTSVDFAVNTEGVYSEPRPIGTRYLTRNL 738
```

Figure 1. Rec2 variant V7 with three amino acid residue substitution on Rec2 capsid

(A) Schematic of V7 trans plasmid.

(B) V7 capsid amino acid sequence with residue substitution highlighted.

V7-based dual adipokines gene therapy rescues metabolic syndromes in congenital leptin deficiency

To investigate the therapeutic potential of V7 vector, we conducted a proof-of-concept study in *ob/ob* mice, a model for congenital leptin deficiency in humans. Previously, we reported that a single injection of AS/Rec2-leptin (4E10 vg/mouse, i.p.) completely rescued the metabolic abnormalities including obesity, hyperphagia, low energy expenditure, fatty liver, glucose intolerance, and hyperinsulinemia.[9] To facilitate clinical translation, we developed a new gene therapy based on the V7 capsid. Because V7 vector ablates liver tropism, the liver-restricting cassette in the AS/Rec2 system becomes unnecessary and therefore avoiding concerns of introducing exogenous regulatory elements that might interfere with endogenous microRNA machinery especially at high expression levels. Moreover, absence of transduction to the liver by V7 vector could minimize the severe adverse events related to liver toxicity that has been a major challenge to the field of systemic gene therapies.[15,16] In addition, AAV gene therapy allows delivery of more than one therapeutic gene. Adiponectin is a major adipokine produced exclusively by adipocytes and plays a crucial role in glucose and lipid metabolism, inflammation, and oxidative stress.[20,21] Adiponectin level is decreased in obesity and lipodystrophy. We hypothesize a gene therapy delivering both leptin and adiponectin will alleviate the metabolic abnormalities in lipodystrophy more efficiently than delivery of leptin alone. We constructed the LEP/ADIPOQ transgene using the 2A sequence to link human leptin cDNA and human adiponectin cDNA. The 2A sequence allows expression of the two adipokines from one transcript. Such design has been successfully applied to the IL15/Il15Rα gene therapy in our previous study.[22] The LEP/ADIPOQ gene was cloned to the ubiquitous CBA expression plasmid and packaged to V7 capsid (Figure 4A).

Male *ob/ob* mice, 7 weeks of age, were randomized to receive an i.p. administration of V7-LEP/ADIPOQ (4E10 vg or 8E10 vg/mouse) or V7-GFP (8E10 vg/mouse). Age-matched male *ob* heterozygote (*ob/+*) from the colony was used as a control for normal metabolic phenotypes. The body weight of *ob/ob* mice receiving V7-GFP were observed to increase rapidly over 9 weeks period of the study (Figures 4B and 4C). In contrast, the weight gain of *ob/ob* mice was leveled off two weeks after injection of V7-LEP/ADIPOQ at both doses (4E10 and 8E10 vg/mouse) (Figures 4B–4E). High dose (8E10 vg/mouse) of V7-LEP/ADIPOQ almost brought the body weight back to the starting point (Figures 4B and 4C). When the weight gain per week was compared among four groups, the LEP/ADIPOQ gene delivery showed a dose dependent effect on restricting body weight gain of *ob/ob* mice (Figure 4E). High dose (8E10 vg/mouse) *ob/ob* group was comparable to heterozygote group over the duration of the study (Figures 4D and 4E), indicating complete rescue of excessive weight gain in *ob/ob* mice. A glucose tolerance test was performed at 7 weeks post AAV injection. V7-LEP/ADIPOQ treatment, both low dose and high dose, completely normalized the fast-state glucose disposal (Figures 4F and 4G). Abnormal low body temperature is a known feature of *ob/ob* mice and can be restored by leptin replacement. It is reported that *ob/ob* mice do not exhibit reduced BAT thermogenic capacity, but thermoregulatory thresholds are shifted downward. Leptin replacement can normalize *ob/ob* body temperature to wildtype mice level by reducing heat loss.[23] V7-LEP/ADIPOQ treatment corrected the abnormal low body temperature of *ob/ob* mice independent of doses (Figure 5A). Body composition was determined by echoMRI at 9 weeks post AAV injection. V7-LEP/ADIPOQ treatment significantly reduced adiposity and increased lean mass compared to *ob/ob* mice treated with V7-GFP, with high dose trending to larger changes of body composition (Figure 5B). Consistent with echoMRI data, at sacrifice 9 weeks after V7 vectors administration, the relative weight of adipose depots, such as eWAT, iWAT, rWAT and BAT in V7-LEP/ADIPOQ mice (both doses) were all reduced significantly compared to *ob/ob* mice treated with V7-GFP ranging from 40% to 70% (Figure 5C). Relative liver mass was reduced by 50% with both doses of V7-LEP/ADIPOQ (Figure 5C).

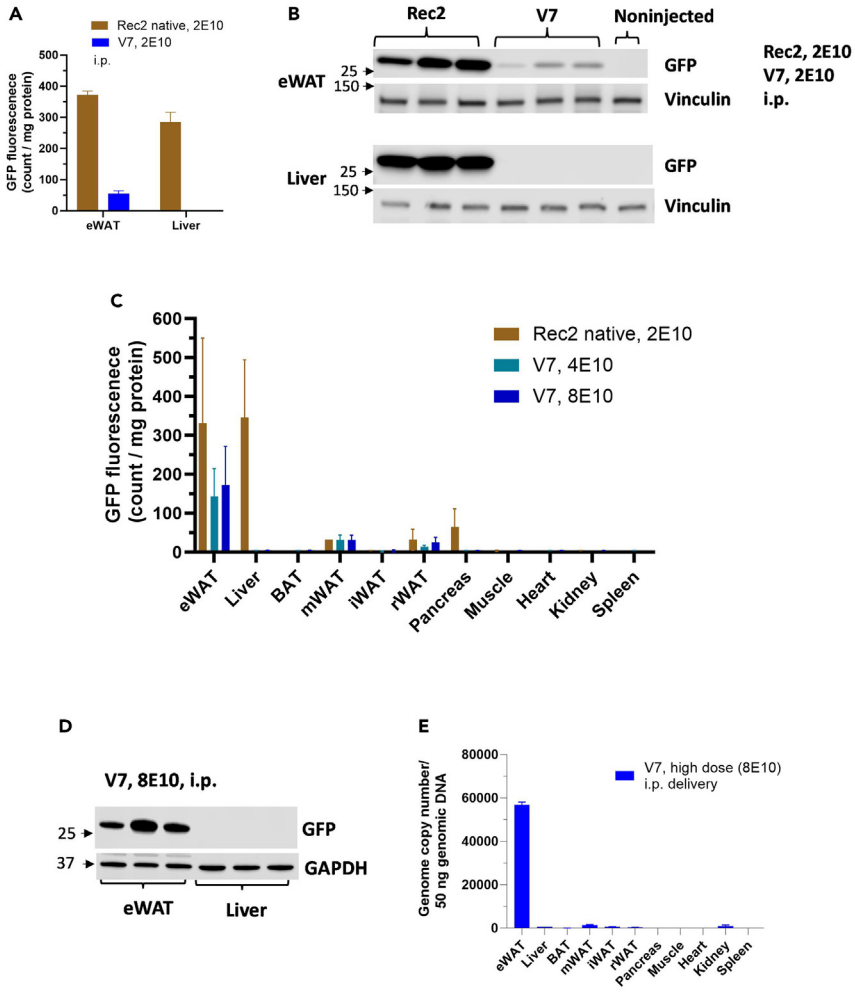

Figure 2. Intraperitoneal administration of V7 vector selectively transduces visceral adipose tissue and de-targets liver

(A) GFP fluorescence in eWAT and liver at 2 weeks post i.p. injection of Rec2-GFP or V7-GFP vectors.

(B) Western blotting in a separate experiment two weeks post AAV injection.

(C) GFP fluorescence in dosing experiment at 2 weeks post i.p. injection.

(D) Western blotting in mice receiving high dose V7-GFP.

(E) Vector genome copy numbers in mice receiving high dose V7-GFP. Doses are indicated in each graph. Data are means ± SEM. Sample size (biological replicates): Rec2-GFP 2E10 vg/mouse n = 3–8, V7-GFP 2E10 vg/mouse n = 8, V7-GFP 4E10/mouse n = 5, V7-GFP 8E10 vg/mouse n = 4.

We examined the biodistribution of the V7-LEP/ADIPOQ vector in major peripheral organs/tissues plus brain of a representative mouse from the *ob/ob* V7-LEP/ADIPOQ 8E10 vg/mouse group by qRT-PCR. The primers were designed to detect human ADIPOQ transgene without cross reaction to mouse *Adipoq*. Human ADIPOQ transgene expression was detected in adipose tissues located exclusively in intraperitoneal cavity, including eWAT, mWAT, and rWAT (Figure S2). No transgene mRNA was detected in brain, liver, or other peripheral organs/tissues (Figure S2). Serum levels of human adipokines were measured with ELISAs without cross reaction to mouse counterparts. The serum levels of human leptin and adiponectin showed a dose dependent effect although not reaching statistical significance (Figure 6A). Human leptin level reached 0.86 ± 0.15 ng/mL and 1.65 ± 0.6 ng/mL with low and high dose, respectively (Figure 6A), a comparable level to that of wildtype mice serum level or Rec2-dual cassette leptin vector,[9] and exceeding the serum level of mouse leptin in the *ob*/+ control mice (0.70 ± 0.05 ng/mL). Human adiponectin serum level was 2.5 ± 0.8 ng/mL and 4.4 ± 2.0 ng/mL with low and high dose, respectively (Figure 6A). *ob/ob* mice exhibited hyperinsulinemia, whose serum insulin levels were robustly reduced by V7-LEP/ADIPOQ treatment ranging from 3 to 9-folds dependent of dose (Figure 6B). Of note, high dose V7-LEP/ADIPOQ brought down serum insulin of *ob/ob* mice to the level comparable to *ob* heterozygote mice. Serum glucose level was also decreased significantly with both doses of V7-LEP/ADIPOQ in comparison to *ob/ob* V7-GFP mice. High dose, in particular, completely normalized serum glucose to the level of *ob* heterozygote mice (Figure 6C). Hepatic triglyceride content was significantly decreased in V7-LEP/ADIPOQ mice, both doses, when compared to *ob/ob* V7-GFP control, indicating liver steatosis was significantly diminished. High dose reduced the hepatic lipid content to a comparable level of *ob* heterozygote mice (Figure 6D).

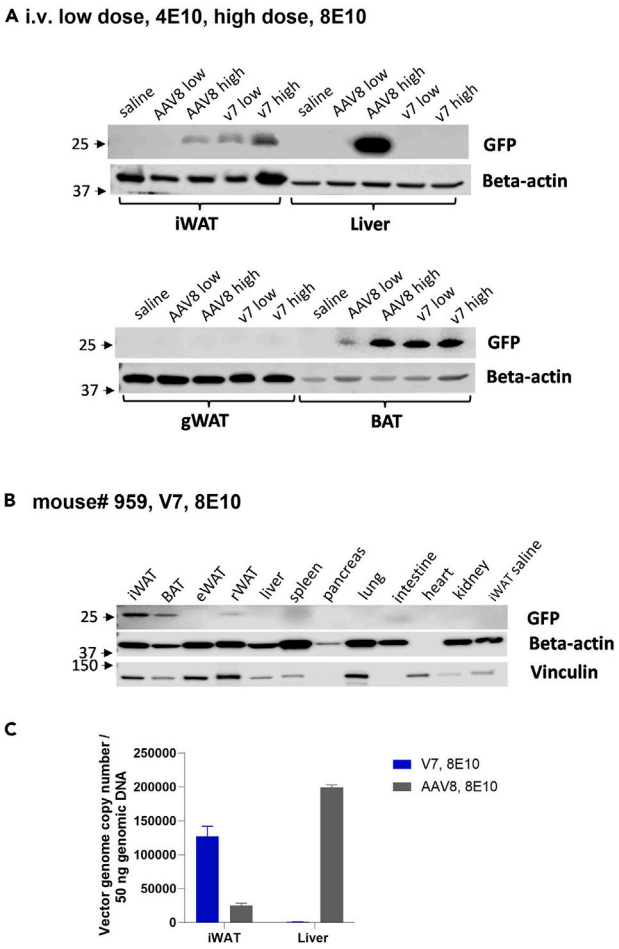

Figure 3. Intravenous injection of V7 vector preferentially transduces subcutaneous white adipose tissue and brown adipose tissue while de-targets liver

(A) Western blotting at 2- weeks post tail vein injection of AAV8-GFP or V7-GFP.

(B) Western blotting of tissues from a mouse receiving V7-GFP (8E10 vg/mouse). Molecular weight markers are shown in kDa.

(C) Vector genome copy numbers in mice receiving high dose of AAV8 or V7-GFP. Doses are indicated in each graph. Data are means ± SEM. Sample size (biological replicates): $n = 3$ per group.

AAV8 capsid with F503Y, Y708D and K709I substitution ablates liver tropism

To investigate whether the mutations in generating V7 capsid are critical for liver-tropism in other AAV capsid, we made the F503Y, Y708D and K709I substitution in AAV8 capsid (Figures 7A and 7B). GFP reporter vector was packaged to the resulting AAV8 mutant capsid as in the V7 experiment and i.p. injected to wildtype mice at the dose of 2E10 vg/mouse. Robust GFP fluorescence was detected in the livers of mice receiving native AAV8 vector while negligible GFP fluorescence was found in the livers of AAV8 mutant vector (Figure 7C). Biodistribution was furtherly assessed by Western blotting. Strong GFP expression in the liver was observed in mice receiving native AAV8, which was completely diminished in mice receiving AAV8 mutant vector even upon extended exposure (Figure 7D). In contrast, GFP was detected in the eWAT of mice receiving AAV8 mutant but at reduced level compared to native AAV8 (Figure 7D).

DISCUSSION

The Rec2 platform has become the leading AAV vector system for adipose gene delivery and has been used by multiple labs worldwide (with or without liver-restricting dual-cassette design).[7,9,10,12–14,22,24–28] However, we are aware of its drawbacks and therefore have put considerable efforts on generating new capsids with improved adipo-tropism while de-targeting liver and other tissues. Here, we demonstrate that the V7 capsid with three mutations (F503Y, Y708D and K709I) on Rec2 capsid achieved selective transduction of adipose tissue while eliminating transgene expression in the liver and other tissues when non-restricted expression cassette was used. The adipo-tropism of the V7 vector were validated by assessments of vector genome, transgene mRNA, and transgene protein. To our knowledge, no AAV capsid that exclusively

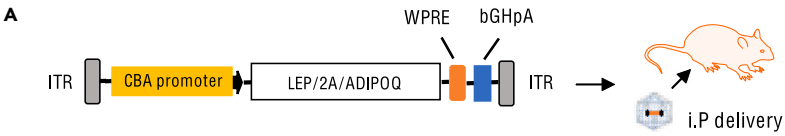
A
WPRE
bGHpA
ITR
CBA promoter
LEP/2A/ADIPOQ
ITR
i.P delivery

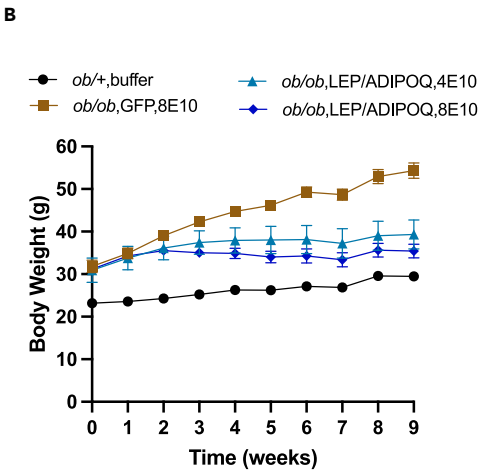
B
ob/+,buffer
ob/ob,GFP,8E10
ob/ob,LEP/ADIPOQ,4E10
ob/ob,LEP/ADIPOQ,8E10
Body Weight (g)
Time (weeks)

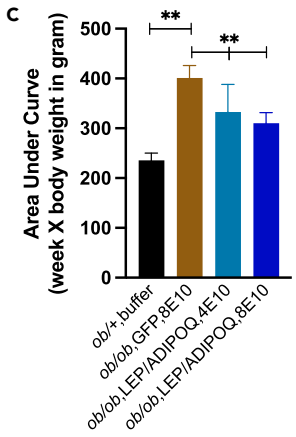
C
Area Under Curve
(week X body weight in gram)
**
**
ob/+,buffer
ob/ob,GFP,8E10
ob/ob,LEP/ADIPOQ,4E10
ob/ob,LEP/ADIPOQ,8E10

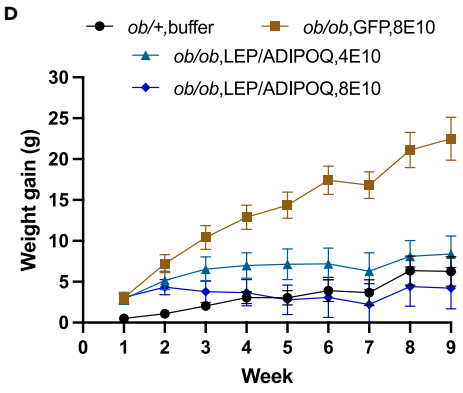
D
ob/+,buffer
ob/ob,GFP,8E10
ob/ob,LEP/ADIPOQ,4E10
ob/ob,LEP/ADIPOQ,8E10
Weight gain (g)
Week

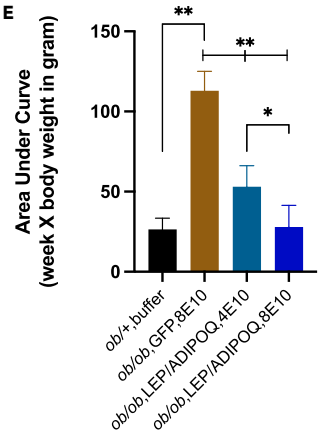
E
Area Under Curve
(week X body weight in gram)
**
**
*
ob/+,buffer
ob/ob,GFP,8E10
ob/ob,LEP/ADIPOQ,4E10
ob/ob,LEP/ADIPOQ,8E10

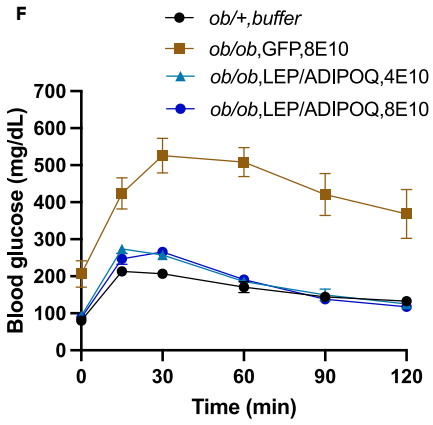
F
ob/+,buffer
ob/ob,GFP,8E10
ob/ob,LEP/ADIPOQ,4E10
ob/ob,LEP/ADIPOQ,8E10
Blood glucose (mg/dL)
Time (min)

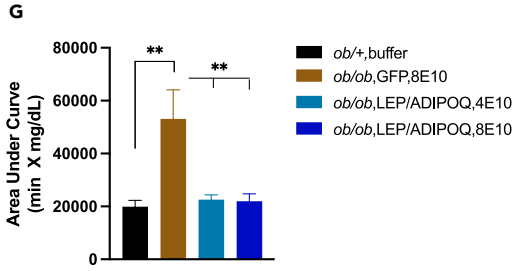
G
Area Under Curve
(min X mg/dL)
**
**
ob/+,buffer
ob/ob,GFP,8E10
ob/ob,LEP/ADIPOQ,4E10
ob/ob,LEP/ADIPOQ,8E10

Figure 4. Intraperitoneal administration of V7-LEP/ADIPOQ vector rescues the excessive weight gain and impaired glycemic control in *ob/ob* mice

(A) Schematic of the AAV vector containing human leptin and human adiponectin linking by 2A sequence.

(B) Body weight.

(C) Area under the curve of body weight.

(D) Weight gain.

(E) Area under the curve of weight gain.

(F) Glucose tolerance test at 8-week post AAV injection.

(G) Area under the curve of glucose tolerance test. Data are means ± SEM. Sample size (biological replicates): *ob*/+ buffer $n = 5$, *ob/ob* GFP 8E10 $n = 5$, *ob/ob* LEP/ADIPOQ 4E10 $n = 4$, *ob/ob* LEP/ADIPOQ 8E10 $n = 4$. *$p < 0.05$, **$p < 0.01$ from one-way ANOVA followed by Tukey's multiple comparison test.

transduces adipose tissue while ablating liver tropism has been reported. As such, the V7 capsid may represent the first of this new class of AAV capsid.

Rec2 vector has shown differential tropism based on delivery route. I.V. administration leads to primarily liver transduction.[8] I.P. injection transduces both liver and visceral WAT.[9] Surprisingly, oral administration of Rec2 transduces the intrascapular BAT but not gastric intestinal track or liver.[29] V7 vector clearly displayed a distinct biodistribution compared to the parent Rec2 capsid. Systemic administration of V7 vector led to no liver transduction while the transduction of fat depots depended on the administration routes: i.p. delivery favoring visceral fat depots while i.v. administration favoring subcutaneous WAT and BAT. The different pattern of fat transduction by i.v. versus i.p. administration is likely attributed to mouse anatomy of adipose tissue and their vasculature. Previous study reported that i.v. administration of AAV8- or AAV9-GFP yielded varying transduction efficiency to fat depots with highest GFP expression in mWAT, BAT and iWAT, and least GFP expression in eWAT. Of note, the doses used for AAV8 or AAV9 vectors were 5E12 vg/mouse,[30] much higher than the dose of 8E10 vg/mouse used in the V7 study. It is possible that increasing dose of V7 vector can improve the transduction of visceral fat by i.v. injection. Alternatively, combining i.v. and i.p. administration may achieve whole body adipose transduction, worthy of further investigation. Future study will also examine whether V7 exhibits altered biodistribution compared to the parent Rec2 capsid via oral administration.

One of the main objectives of this study was to eliminate the liver tropism of Rec2 capsid. Rec2 is a chimeric capsid generated via shuffling between capsid of AAV8 and rh20.[6] AAV8 and rh20 have been shown to efficiently transduce liver[19] and brain tissue,[31] respectively. We analyzed amino acid sequence of capsid among AAV2, 8, 9, Rec2, Rec3, and chose the locations to make point mutations or insertional mutation in Rec2 capsid based on the functional readout data in the publications for AAV2 capsid residues.[1,5,32–36] *Capsid (cap)* gene encodes structural viral proteins VP1-3 via an alternative splicing and initiation. All three VP proteins share identical carboxyl-terminal amino acids. Tissue tropism of AAV depends on the specific interactions between capsid-specific structures and cellular glycans and receptors. AAV2 makes a cell entry by using membrane-associated heparan sulfate proteoglycan (HSPG) as its primary receptor. Other candidates have also been reported to participate AAV attachment. The atomic structure of AAV2 capsid has been determined at a resolution of 3.0 micron.[35] Based on the computer modeling, some genetic capsid modifications can be tolerated for AAV2 capsid. For example, previous work suggested potential heparin binding loci that include a cluster between position 561 and 591, which was re-confirmed by recent comprehensive AAV capsid fitness landscape study.[5] Further studies identify residues R585 and R588 as two primary residues responsible for HSPG binding.[32] Additional studies report genetic mutation on position 587 and surrounding residues for vector re-targeting,[37] and map some of amino acid residues at extreme C-terminus, which is essential for liver transduction by AAV2 and AAV9.[35,38] Thus, we decided to make mutations on Rec2 capsid in the region equivalent to the region surrounding R585 and R588 of AAV2 capsid and to screen new capsids with adipose tropism and de-targeting liver. Additional modifications were expanded beyond the R585∼R588 region (Table S1). Only one variant V7 made the cut—maintaining adipo-tropism while ablating liver tropism suggesting that the design rationales might not work out and the trial-and-error method remains necessary. Regarding liver transduction, the F503Y, Y708D and K709I substitution resulted in ablating liver tropism in both Rec2 and AAV8 capsids suggesting F503, Y708 and K709 together play a critical role in hepatic transduction of Rec2 and AAV8 vectors. We are testing whether these substitutions can be applied to additional commonly used AAV capsids such as AAV9. Notably, although being able to maintain adipo-tropism, the efficiency of V7 capsid was lower than Rec2 capsid but still higher than AAV8. We speculate that the domains in Rec2 capsid critical for the vector entry into adipose tissue and liver likely reside at C-terminal of VP of Rec2 capsid and are possibly overlapped partially. As such, when the three-residue substitution (F503Y/Y708D/K709I) disrupts liver binding, it likely affects adipose binding domain as well. Future work will use V7 as the template for capsid modification to improve adipo-tropism.

In addition to serving as a tool for basic research on adipose biology, adipo-tropic AAV vectors can provide an avenue to developing gene therapies for genetic disorders and disease conditions involving adipose tissue. The pathology of adipose tissue is most often associated with obesity or diabetes in humans. Six forms of human monogenic obesity are primarily due to inactivating mutations in leptin-melanocortin signaling.[4] Congenital leptin deficiency is a monogenic defect found in adipose tissue,[39] causing severe obesity, hyperphagia, and hyperinsulinemia. Moreover, leptin deficiency shares many symptoms with lipodystrophy. Leptin replacement therapy is necessary in patients with homozygous leptin mutations or acquired leptin deficiency derived from congenital or acquired lipodystrophy.[40–42] Recombinant leptin protein analog (metreleptin) is an approved drug but requires frequent injection for life and cost an average of $565,000 per patient per year. Gene therapy based on an adipo-tropic AAV vector may have significant advantages compared to current standard of care. Our adipo-tropic AAV platform has the potential to enabling lower overall systemic doses to patients, resulting in fewer toxicities and much lower cost of goods for systemically delivered gene therapies.

Our prior preclinical study has demonstrated this potential using the Rec2/dual cassette vector in *ob/ob* mice.[9] Here, we conducted a proof-of-concept for a V7-based gene therapy in the *ob/ob* mice mirroring the published study. A single i.p. injection of V7 vector carrying

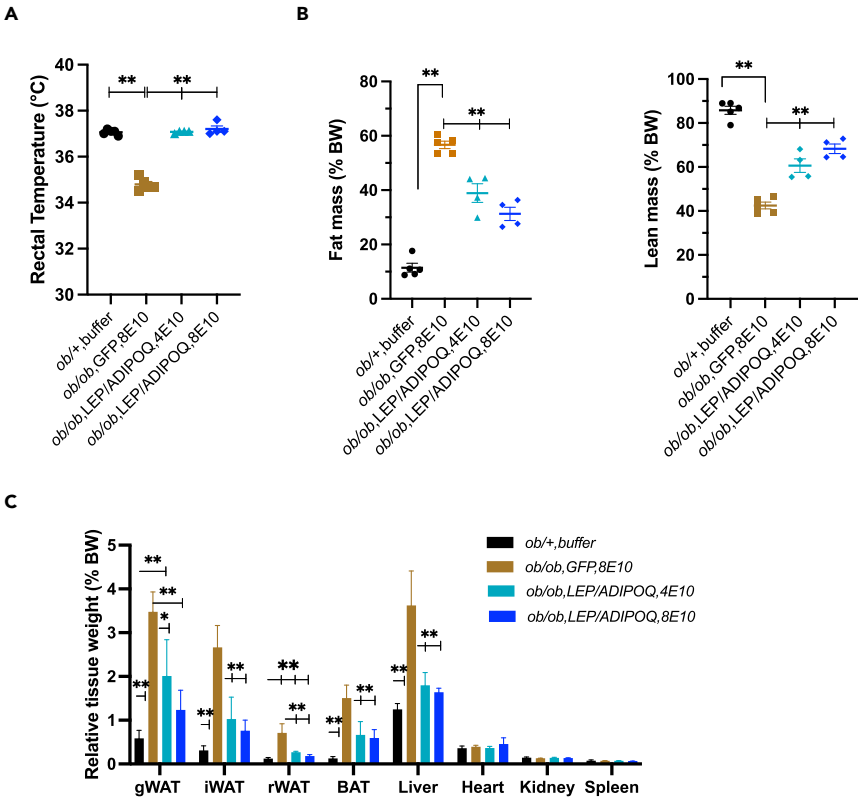

Figure 5. Intraperitoneal administration of V7-LEP/ADIPOQ vector normalizes body temperature and body composition in *ob/ob* mice

(A) Rectal temperature at 8-week post AAV injection.

(B) Body composition by Echo MRI at 9 week post AAV injection.

(C) Relative tissue mass calibrated to body weight at sacrifice 9 weeks post AAV injection. Data are means ± SEM. Sample size (biological replicates): *ob/+* buffer $n = 5$, *ob/ob* GFP 8E10 $n = 5$, *ob/ob* LEP/ADIPOQ 4E10 $n = 4$, *ob/ob* LEP/ADIPOQ 8E10 $n = 4$. *$p < 0.05$, **$p < 0.01$ from One-way ANOVA followed by Tukey's multiple comparison test.

human leptin and human adiponectin normalized excessive weight gain, glucose intolerance, abnormal low core temperature, hyperinsulinemia, and hepatic steatosis in the *ob/ob* mice. Noteworthy, V7 vector at the low dose of 4E10 vg/mouse resulted in the circulating level of human leptin comparable to the normal level of mouse leptin in WT mice.[9] Importantly, the dose of V7 vector was 50–100-folds lower than standard gene therapies but achieved higher level of leptin expression.[9,43] Because restoring the circulating leptin level to 10% of normal levels is sufficient to mitigate the metabolic syndromes associated with congenital leptin deficiency,[43] the dose of V7-LEP/ADIPOQ could be further reduced. Moreover, we hypothesize that a gene therapy delivering both leptin and adiponectin will alleviate the metabolic abnormalities more efficiently than leptin alone in lipodystrophy models because adiponectin promotes adipogenesis.[44] Future research will assess the therapeutic efficacy of V7-LEP/ADIPOQ in seipin-deficient mice and caveolin-deficient mice that are highly relevant to human lipodystrophy.[45,46]

In summary, our data demonstrate that the engineered Rec2 capsid variant V7 with F503Y, Y708D, and K709I substitution achieved selective transduction to adipose tissue and ablating liver tropism upon systemic administration in mice. These substitutions can be applied to AAV8 capsid for liver de-targeting indicating F503, Y708 and K709 critical for liver transduction. A single administration of V7-LEP/ADIPOQ led to reversal of metabolic abnormalities in a murine model of congenital leptin deficiency at a dose substantially lower than those commonly used for AAV systemic gene therapy. Further characterization and refinement of V7 vector platform will provide a powerful tool kit enabling genetic manipulation of adipose tissue in basic research and gene therapy for adipose-originated diseases and beyond.

Limitation of the study

There are limitations for the current study and further characterization of the V7 capsid is required to provide a comprehensive user manual. Studies are underway to determine the percentage of adipocytes being transduced by V7 vector and whether V7 vector can transduce other cell populations residing in the adipose tissue (e.g., immune cells and progenitor cells) that are critical for some applications such as knockdown endogenous adipose genes and investigations on interaction between mature adipocytes and stromal vascular fraction (SVF). In a preliminary study, we isolated mature adipocytes and SVF from eWAT of mice receiving IP injection of V7-GFP (8E10 vg/mouse) and performed

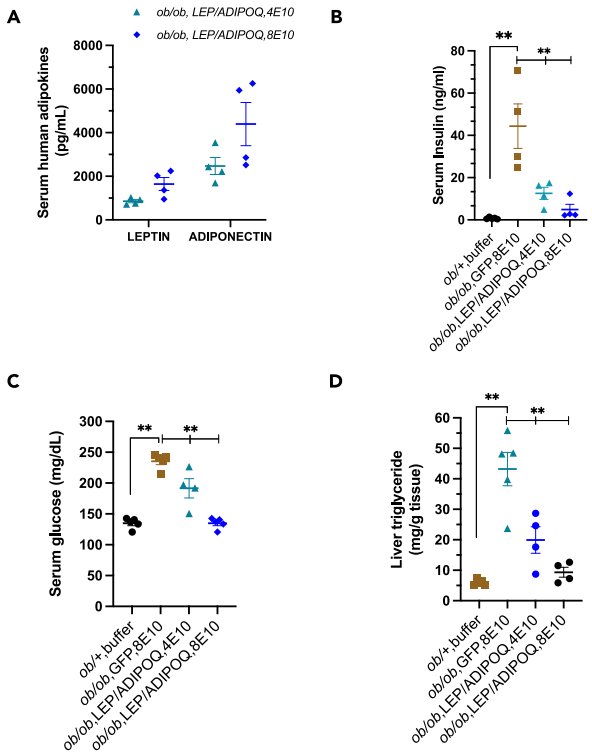

Figure 6. Intraperitoneal administration of V7-LEP/ADIPOQ reverses hyperinsulinemia, hyperglycemia, and hepatic steatosis in *ob/ob* mice

(A) Serum levels of human leptin and human adiponectin. No significant difference between the low dose and high dose.

(B) Serum level of insulin.

(C) Serum level of glucose.

(D) Liver triglyceride content. Data are means ± SEM. Sample size (biological replicates): *ob*/+ buffer $n = 5$, *ob/ob* GFP 8E10 $n = 5$, *ob/ob* LEP/ADIPOQ 4E10 $n = 4$, *ob/ob* LEP/ADIPOQ 8E10 $n = 4$. *$p < 0.05$, **$p < 0.01$ from One-way ANOVA followed by Tukey's multiple comparison test.

qRT-PCR to quantify GFP mRNA. The majority of GFP mRNA was detected in the mature adipocytes while the GFP expression in SVF was 4.4% of that in the mature adipocytes, suggesting V7 vector mainly transduces mature adipocytes. The preliminary findings will be validated by flow cytometry and immunohistochemistry in future studies. Moreover, ablating liver tropism of V7 capsid presumably reduces viral vector-associated toxicity. Because severe adverse events were rarely observed in clinical and nonclinical studies and mostly occurred after administration of very high dose (>1 to 3E14 vg/kg i.v.),[15,16] our current study using low doses (<3E12 vg/kg) was unable to assess toxicity. We plan to conduct a dose-escalating experiment to assess immunogenicity and general toxicity of V7 with AAV8 as the reference capsid. Admittedly, biodistribution of transgene mRNA was obtained from one representative mouse of V7-LEP/ADIPOQ 8E10 group (Figure S2). Adding more biological replicates will further validate the data. Another limitation is that all *in vivo* data were obtained in mice. Testing in other species, particularly nonhuman primates, is required to assess the translatability of this adipo-tropic AAV capsid.

RESOURCE AVAILABILITY

Lead contact

Further information and requests for resources and reagents should be directed to and will be fulfilled by the lead contact, Lei Cao (lei.cao@osumc.edu).

Materials availability

Requests for AAV capsids should be directed to the lead contact, Lei Cao (lei.cao@osumc.edu).

Data and code availability

- All data reported in this paper will be shared by the lead contact upon request.
- This paper does not report original code.
- Any additional information required to reanalyze the data reported in this paper is available from the lead contact upon request.

ACKNOWLEDGMENTS

This work was supported by NIH grants CA166590, DK137431, and internal funding from The Ohio State University Comprehensive Cancer Center.

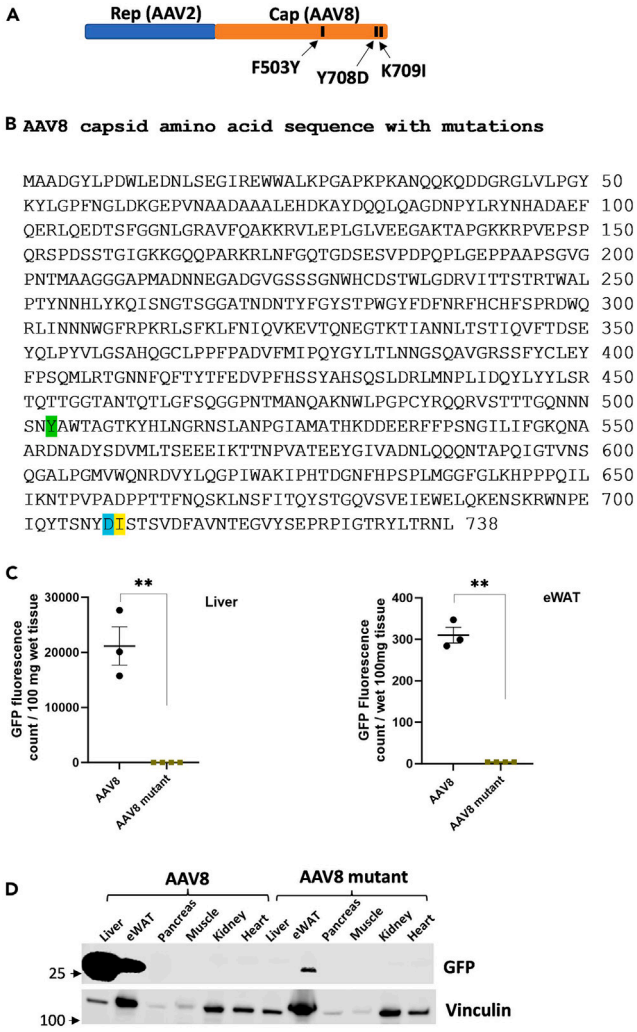

Figure 7. AAV8 capsid with F503Y/Y708D/K709I substitution loses liver-tropism

(A) Schematic of AAV8 mutant trans plasmid.

(B) AAV8 mutant capsid amino acid sequence with residue substitution highlighted.

(C) GFP fluorescence in liver and eWAT at 2-week post i.p. injection of AAV8 or AAV8 mutant vector at 2E10 vg/mouse. Data are means ± SEM. Sample size (biological replicates): AAV8 $n = 3$, AAV8 mutant $n = 4$. $^{**}p < 0.01$ from Student t test.

(D) Western blotting of GFP in various tissues upon extended exposure. Molecular weight markers are shown in kDa.

AUTHOR CONTRIBUTIONS

Conceptualization, W.H. and L.C.; Methodology, W.H. and L.C.; Validation, W.H. and L.C.; Investigation, W.H., R.B., B.A., T.M., and L.C.; Resources, W.H. and L.C.; Data Curation, W.H. and L.C.; Writing, W.H. and L.C.; Funding Acquisition, L.C.

DECLARATION OF INTERESTS

L.C. and W.H. are inventors of provisional US patent application #63/583,110. L.C. is co-founder of Zvelt Therapeutics to which the provisional patent is licensed. Other authors declare no competing financial interests.

STAR★METHODS

Detailed methods are provided in the online version of this paper and include the following:

- KEY RESOURCES TABLE
- EXPERIMENTAL MODEL AND STUDY PARTICIPANT DETAILS
  - Mice
- METHOD DETAILS
  - Capsid modifications by site-directed mutagenesis

SUPPLEMENTAL INFORMATION

Supplemental information can be found online at https://doi.org/10.1016/j.isci.2024.110930.

Received: January 12, 2024
Revised: April 8, 2024
Accepted: September 9, 2024
Published: September 17, 2024

REFERENCES

1. Büning, H., and Srivastava, A. (2019). Capsid modifications for targeting and improving the efficacy of AAV vectors. Mol. Ther. Methods Clin. Dev. *12*, 248–265. https://doi.org/10.1016/j.omtm.2019.01.008.
2. Pupo, A., Fernández, A., Low, S.H., Francois, A., Suárez-Amarán, L., and Samulski, R.J. (2022). AAV vectors: The Rubik's cube of human gene therapy. Mol. Ther. *30*, 3515–3541. https://doi.org/10.1016/j.ymthe.2022.09.015.
3. Mingozzi, F., and High, K.A. (2011). Therapeutic *in vivo* gene transfer for genetic disease using AAV: progress and challenges. Nat. Rev. Genet. *12*, 341–355. https://doi.org/10.1038/nrg2988.
4. Bates, R., Huang, W., and Cao, L. (2020). Adipose Tissue: An Emerging Target for Adeno-associated Viral Vectors. Mol. Ther. Methods Clin. Dev. *19*, 236–249. https://doi.org/10.1016/j.omtm.2020.09.009.
5. Ogden, P.J., Kelsic, E.D., Sinai, S., and Church, G.M. (2019). Comprehensive AAV capsid fitness landscape reveals a viral gene and enables machine-guided design. Science *366*, 1139–1143. https://doi.org/10.1126/science.aaw2900.
6. Charbel Issa, P., De Silva, S.R., Lipinski, D.M., Singh, M.S., Mouravlev, A., You, Q., Barnard, A.R., Hankins, M.W., During, M.J., and Maclaren, R.E. (2013). Assessment of tropism and effectiveness of new primate-derived hybrid recombinant AAV serotypes in the mouse and primate retina. PLoS One *8*, e60361. https://doi.org/10.1371/journal.pone.0060361.
7. Liu, X., Magee, D., Wang, C., McMurphy, T., Slater, A., During, M., and Cao, L. (2014). Adipose tissue insulin receptor knockdown via a new primate-derived hybrid recombinant AAV serotype. Mol. Ther. Methods Clin. Dev. *1*, 8. https://doi.org/10.1038/mtm.2013.8.
8. McMurphy, T.B., Huang, W., Xiao, R., Liu, X., Dhurandhar, N.V., and Cao, L. (2017). Hepatic Expression of Adenovirus 36 E4ORF1 Improves Glycemic Control and Promotes Glucose Metabolism Through AKT Activation. Diabetes *66*, 358–371. https://doi.org/10.2337/db16-0876.
9. Huang, W., Liu, X., Queen, N.J., and Cao, L. (2017). Targeting Visceral Fat by Intraperitoneal Delivery of Novel AAV Serotype Vector Restricting Off-Target Transduction in Liver. Mol. Ther. Methods Clin. Dev. *6*, 68–78. https://doi.org/10.1016/j.omtm.2017.06.002.
10. Huang, W., Queen, N.J., McMurphy, T.B., Ali, S., and Cao, L. (2019). Adipose PTEN regulates adult adipose tissue homeostasis and redistribution via a PTEN-leptin-sympathetic loop. Mol. Metabol. *30*, 48–60. https://doi.org/10.1016/j.molmet.2019.09.008.
11. Huang, W., Queen, N.J., McMurphy, T.B., Ali, S., Wilkins, R.K., Appana, B., and Cao, L. (2020). Adipose PTEN acts as a downstream mediator of a brain-fat axis in environmental enrichment. Compr. Psychoneuroendocrinol. *4*, 100013. https://doi.org/10.1016/j.cpnec.2020.100013.
12. Queen, N.J., Bates, R., Huang, W., Xiao, R., Appana, B., and Cao, L. (2021). Visceral adipose tissue-directed FGF21 gene therapy improves metabolic and immune health in BTBR mice. Mol. Ther. Methods Clin. Dev. *20*, 409–422. https://doi.org/10.1016/j.omtm.2020.12.011.
13. Xiao, R., Mansour, A.G., Huang, W., Hassan, Q.N., 2nd, Wilkins, R.K., Komatineni, S.V., Bates, R., Ali, S., Chrislip, L.A., Queen, N.J., et al. (2022). Adipocyte CD1d Gene Transfer Induces T Cell Expansion and Adipocyte Inflammation in CD1d Knockout Mice. J. Immunol. *208*, 2109–2121. https://doi.org/10.4049/jimmunol.2100313.
14. Morató, L., Astori, S., Zalachoras, I., Rodrigues, J., Ghosal, S., Huang, W., Guillot de Suduiraut, I., Grosse, J., Zanoletti, O., Cao, L., et al. (2022). eNAMPT actions through nucleus accumbens NAD(+)/SIRT1 link increased adiposity with sociability deficits programmed by peripuberty stress. Sci. Adv. *8*, eabj9109. https://doi.org/10.1126/sciadv.abj9109.
15. Yang, T.Y., Braun, M., Lembke, W., McBlane, F., Kamerud, J., DeWall, S., Tarcsa, E., Fang, X., Hofer, L., Kavita, U., et al. (2022). Immunogenicity assessment of AAV-based gene therapies: An IQ consortium industry white paper. Mol. Ther. Methods Clin. Dev. *26*, 471–494. https://doi.org/10.1016/j.omtm.2022.07.018.
16. Verdera, H.C., Kuranda, K., and Mingozzi, F. (2020). AAV Vector Immunogenicity in Humans: A Long Journey to Successful Gene Transfer. Mol. Ther. *28*, 723–746. https://doi.org/10.1016/j.ymthe.2019.12.010.
17. Anderson, J.M., Arnold, W.D., Huang, W., Ray, A., Owendoff, G., and Cao, L. (2024). Long-term effects of a fat-directed FGF21 gene therapy in aged female mice. Gene Ther. *31*, 95–104. https://doi.org/10.1038/s41434-023-00422-0.
18. Dhungel, B.P., Bailey, C.G., and Rasko, J.E.J. (2021). Journey to the Center of the Cell: Tracing the Path of AAV Transduction. Trends Mol. Med. *27*, 172–184. https://doi.org/10.1016/j.molmed.2020.09.010.
19. Gao, G.P., Alvira, M.R., Wang, L., Calcedo, R., Johnston, J., and Wilson, J.M. (2002). Novel adeno-associated viruses from rhesus monkeys as vectors for human gene therapy. Proc. Natl. Acad. Sci. USA *99*, 11854–11859. https://doi.org/10.1073/pnas.182412299.
20. Kadowaki, T., Yamauchi, T., Kubota, N., Hara, K., Ueki, K., and Tobe, K. (2006). Adiponectin and adiponectin receptors in insulin resistance, diabetes, and the metabolic syndrome. J. Clin. Invest. *116*, 1784–1792. https://doi.org/10.1172/JCI29126.
21. Kita, S., Maeda, N., and Shimomura, I. (2019). Interorgan communication by exosomes, adipose tissue, and adiponectin in metabolic syndrome. J. Clin. Invest. *129*, 4041–4049. https://doi.org/10.1172/JCI129193.
22. Xiao, R., Mansour, A.G., Huang, W., Chrislip, L.A., Wilkins, R.K., Queen, N.J., Youssef, Y., Mao, H.C., Caligiuri, M.A., and Cao, L. (2019). Adipocytes: a novel target for IL-15/IL-15R alpha cancer gene therapy. Mol. Ther. *27*, 922–932. https://doi.org/10.1016/j.ymthe.2019.02.011.
23. Fischer, A.W., Hoefig, C.S., Abreu-Vieira, G., de Jong, J.M.A., Petrovic, N., Mittag, J., Cannon, B., and Nedergaard, J. (2016). Leptin Raises Defended Body Temperature without Activating Thermogenesis. Cell Rep. *14*, 1621–1631. https://doi.org/10.1016/j.celrep.2016.01.041.
24. Wagner, G., Fenzl, A., Lindroos-Christensen, J., Einwallner, E., Husa, J., Witzeneder, N., Rauscher, S., Gröger, M., Derdak, S., Mohr, T., et al. (2021). LMO3 reprograms visceral adipocyte metabolism during obesity. J. Mol. Med. *99*, 1151–1171. https://doi.org/10.1007/s00109-021-02089-9.
25. Zhang, Y., Xie, L., Gunasekar, S.K., Tong, D., Mishra, A., Gibson, W.J., Wang, C., Fidler, T., Marthaler, B., Klingelhutz, A., et al. (2017). SWELL1 is a regulator of adipocyte size, insulin signalling and glucose homeostasis. Nat. Cell Biol. *19*, 504–517. https://doi.org/10.1038/ncb3514.
26. Xie, L., Zhang, Y., Gunasekar, S.K., Mishra, A., Cao, L., and Sah, R. (2017). Induction of adipose and hepatic SWELL1 expression is required for maintaining systemic insulin-sensitivity in obesity. Channels *11*, 673–677. https://doi.org/10.1080/19336950.2017.1373225.
27. Ng, R., Hussain, N.A., Zhang, Q., Chang, C., Li, H., Fu, Y., Cao, L., Han, W., Stunkel, W., and Xu, F. (2017). miRNA-32 Drives Brown Fat Thermogenesis and Trans-activates Subcutaneous White Fat Browning in Mice. Cell Rep. *19*, 1229–1246. https://doi.org/10.1016/j.celrep.2017.04.035.
28. Zhu, Y., Gao, Y., Tao, C., Shao, M., Zhao, S., Huang, W., Yao, T., Johnson, J.A., Liu, T., Cypess, A.M., et al. (2016). Connexin 43 Mediates White Adipose Tissue Beiging by Facilitating the Propagation of Sympathetic

Neuronal Signals. Cell Metabol. *24*, 420–433. https://doi.org/10.1016/j.cmet.2016.08.005.

29. Huang, W., McMurphy, T., Liu, X., Wang, C., and Cao, L. (2016). Genetic Manipulation of Brown Fat Via Oral Administration of an Engineered Recombinant Adeno-associated Viral Serotype Vector. Mol. Ther. *24*, 1062–1069. https://doi.org/10.1038/mt.2016.34.
30. Jimenez, V., Muñoz, S., Casana, E., Mallol, C., Elias, I., Jambrina, C., Ribera, A., Ferre, T., Franckhauser, S., and Bosch, F. (2013). In vivo adeno-associated viral vector-mediated genetic engineering of white and brown adipose tissue in adult mice. Diabetes *62*, 4012–4022. https://doi.org/10.2337/db13-0311.
31. Lawlor, P.A., Bland, R.J., Mouravlev, A., Young, D., and During, M.J. (2009). Efficient gene delivery and selective transduction of glial cells in the mammalian brain by AAV serotypes isolated from nonhuman primates. Mol. Ther. *17*, 1692–1702. https://doi.org/10.1038/mt.2009.170.
32. Kern, A., Schmidt, K., Leder, C., Müller, O.J., Wobus, C.E., Bettinger, K., Von der Lieth, C.W., King, J.A., and Kleinschmidt, J.A. (2003). Identification of a heparin-binding motif on adeno-associated virus type 2 capsids. J. Virol. *77*, 11072–11081. https://doi.org/10.1128/jvi.77.20.11072-11081.2003.
33. Zhang, R., Cao, L., Cui, M., Sun, Z., Hu, M., Zhang, R., Stuart, W., Zhao, X., Yang, Z., Li, X., et al. (2019). Adeno-associated virus 2 bound to its cellular receptor AAVR. Nat. Microbiol. *4*, 675–682. https://doi.org/10.1038/s41564-018-0356-7.
34. Zhong, L., Li, B., Jayandharan, G., Mah, C.S., Govindasamy, L., Agbandje-McKenna, M., Herzog, R.W., Weigel-Van Aken, K.A., Hobbs, J.A., Zolotukhin, S., et al. (2008). Tyrosine-phosphorylation of AAV2 vectors and its consequences on viral intracellular trafficking and transgene expression. Virology *381*, 194–202. https://doi.org/10.1016/j.virol.2008.08.027.
35. Meyer, N.L., Hu, G., Davulcu, O., Xie, Q., Noble, A.J., Yoshioka, C., Gingerich, D.S., Trzynka, A., David, L., Stagg, S.M., and Chapman, M.S. (2019). Structure of the gene therapy vector, adeno-associated virus with its cell receptor,AAVR. Elife *8*, e44707. https://doi.org/10.7554/eLife.44707.
36. Zhong, L., Li, B., Mah, C.S., Govindasamy, L., Agbandje-McKenna, M., Cooper, M., Herzog, R.W., Zolotukhin, I., Warrington, K.H., Jr., Weigel-Van Aken, K.A., et al. (2008). Next generation of adeno-associated virus 2 vectors: point mutations in tyrosines lead to high-efficiency transduction at lower doses. Proc. Natl. Acad. Sci. USA *105*, 7827–7832. https://doi.org/10.1073/pnas.0802866105.
37. Büning, H., Huber, A., Zhang, L., Meumann, N., and Hacker, U. (2015). Engineering the AAV capsid to optimize vector-host-interactions. Curr. Opin. Pharmacol. *24*, 94–104. https://doi.org/10.1016/j.coph.2015.08.002.
38. Adachi, K., Enoki, T., Kawano, Y., Veraz, M., and Nakai, H. (2014). Drawing a high-resolution functional map of adeno-associated virus capsid by massively parallel sequencing. Nat. Commun. *5*, 3075. https://doi.org/10.1038/ncomms4075.
39. Montague, C.T., Farooqi, I.S., Whitehead, J.P., Soos, M.A., Rau, H., Wareham, N.J., Sewter, C.P., Digby, J.E., Mohammed, S.N., Hurst, J.A., et al. (1997). Congenital leptin deficiency is associated with severe early-onset obesity in humans. Nature *387*, 903–908. https://doi.org/10.1038/43185.
40. Farooqi, I.S., Matarese, G., Lord, G.M., Keogh, J.M., Lawrence, E., Agwu, C., Sanna, V., Jebb, S.A., Perna, F., Fontana, S., et al. (2002). Beneficial effects of leptin on obesity, T cell hyporesponsiveness, and neuroendocrine/metabolic dysfunction of human congenital leptin deficiency. J. Clin. Invest. *110*, 1093–1103. https://doi.org/10.1172/JCI15693.
41. Gibson, W.T., Farooqi, I.S., Moreau, M., DePaoli, A.M., Lawrence, E., O'Rahilly, S., and Trussell, R.A. (2004). Congenital leptin deficiency due to homozygosity for the Delta133G mutation: report of another case and evaluation of response to four years of leptin therapy. J. Clin. Endocrinol. Metab. *89*, 4821–4826. https://doi.org/10.1210/jc.2004-0376.
42. Oral, E.A., Simha, V., Ruiz, E., Andewelt, A., Premkumar, A., Snell, P., Wagner, A.J., DePaoli, A.M., Reitman, M.L., Taylor, S.I., et al. (2002). Leptin-replacement therapy for lipodystrophy. N. Engl. J. Med. *346*, 570–578. https://doi.org/10.1056/NEJMoa012437.
43. O'Neill, S.M., Hinkle, C., Chen, S.J., Sandhu, A., Hovhannisyan, R., Stephan, S., Lagor, W.R., Ahima, R.S., Johnston, J.C., and Reilly, M.P. (2014). Targeting adipose tissue via systemic gene therapy. Gene Ther. *21*, 653–661. https://doi.org/10.1038/gt.2014.38.
44. Kim, J.Y., van de Wall, E., Laplante, M., Azzara, A., Trujillo, M.E., Hofmann, S.M., Schraw, T., Durand, J.L., Li, H., Li, G., et al. (2007). Obesity-associated improvements in metabolic profile through expansion of adipose tissue. J. Clin. Invest. *117*, 2621–2637. https://doi.org/10.1172/JCI31021.
45. Garg, A. (2011). Clinical review#: Lipodystrophies: genetic and acquired body fat disorders. J. Clin. Endocrinol. Metab. *96*, 3313–3325. https://doi.org/10.1210/jc.2011-1159.
46. Magré, J., and Prieur, X. (2022). Seipin Deficiency as a Model of Severe Adipocyte Dysfunction: Lessons from Rodent Models and Teaching for Human Disease. Int. J. Mol. Sci. *23*, 740. https://doi.org/10.3390/ijms23020740.
47. Huang, W., Queen, N.J., and Cao, L. (2019). rAAV-Mediated Gene Delivery to Adipose Tissue. Methods Mol. Biol. *1950*, 389–405. https://doi.org/10.1007/978-1-4939-9139-6_23.

STAR★METHODS

KEY RESOURCES TABLE

REAGENT or RESOURCE	SOURCE	IDENTIFIER
Antibodies		
Vinculin (E1E9V)	Cell Signaling Technology	Cat#13901S; RRID: AB_2728768
GFP (B-2) HRP	Santa Cruz Biotechnology	Cat#Sc-9996; RRID: AB_627695
Anti-GAPDH mouse mAb (6C5)	EMD Millipore Corp	Cat#CB1001-500UG
RIPA buffer	Pierce	REF#89901
Chemicals, peptides, and recombinant proteins		
PowerUp SYBR Green Master Mix	Applied Biosystems	REF#A25742
Phosstop	Roche	REF#04906837001
Protease inhibitor cocktail set III, EDTA free	Calbiochem	Cat#539134-1SET
Critical commercial assays		
Human Leptin ELISA	R&D System	Cat#DY398
Human Adiponectin/Acrp30 ELISA	R&D System	Cat#DY1065
Mouse Leptin ELISA	R&D System	Cat#DY498
Mouse Ultrasensitive Insulin ELISA	ALPCO	Cat#80-INSMSU-E01
Triglycerides Colorimetric Assay	Cayman Chemical	Cat#10010303
Glucose Colorimetric Assay	Cayman Chemical	Cat#10009582
GeneArt site-directed mutagenesis Plus kit	Invitrogen	Cat#A14604
RNeasy Mini kit	QIAGEN	Cat#74106
Taqman Reverse Transcription Reagents	Applied Biosystems	Cat#N8080234
DNeasy Blood and Tissue kit	QIAGEN	Cat#69506
Experimental models: Organisms/strains		
Mouse: C57BL/6	Charles River Laboratories	Strain code:027
Mouse: *ob/ob* homozygote	Jackson Laboratories	Strain # 000632
Mouse: *ob/+* heterozygote	Jackson Laboratories	Strain # 000632
Software and algorithms		
GraphPad Prism 9.0	https://www.graphpad.com/	N/A
Microsoft Excel	https://www.microsoft.com/en-us/microsoft-365/excel	N/A

EXPERIMENTAL MODEL AND STUDY PARTICIPANT DETAILS

Mice

Wildtype C57/BL6 mice, 12-18 weeks of age, were purchased from Charles River Laboratories. 7-week-old *ob/ob* mice on a C57/BL6 background were purchased from Jackson Laboratories. All mice were housed in a temperature-controlled room (20-23°C) with a 12-hr. light /12 hr. dark cycle. Mice were maintained on a standard chow diet (7912 rodent chow, Teklad), with free access to food and water *ad libitum*. Male mice were used in all studies. All use of animal was approved and in accordance with the Ohio State University Animal Care and Use Committee (IACUC), protocol approval 2012A00000060-R3.

METHOD DETAILS

Capsid modifications by site-directed mutagenesis

Rec2 capsid V7 mutagenesis

The Rec2 capsid was mutagenized at sites indicated in Figure 1A and full capsid sequence is listed in Figure 1B. We name Rec2 variants as V1 to V8 in numerical order. GeneArt site-directed mutagenesis Plus kit (A14604, Invitrogen) was used to carry out the designated mutagenesis. Rec2 capsid sequence is based on published data.[6] Primers for mutagenesis was synthesized by Sigma-Aldrich: F503Y

(ACAACAATAGCAACTATGCCTGGACTGCTGG, CCAGCAGTCCAGGCATAGTTGCTATTGTTGT); Y708D and K709I (TACACCTCCAAC TACGACATATCTACAAGTGTGGA, TCCACACTTGTAGATATGTCGTAGTTGGAGGTGTA).

Mutagenesis was set up and carried out according to the manufacturer's instruction, and the nucleotide replacement at each site was confirmed by sequencing at the Core Facility of The Ohio State University, Comprehensive Cancer Center. The whole capsid was also sequenced and confirmed without unintended mutation.

AAV8 capsid mutation

Rec2 capsid was generated from capsid domain shuffling between rh20 and AAV8[6] whose C-terminal including those three amino acids mutagenized for V7 is identical to AAV8 capsid C-terminal. As such, AAV8 capsid mutagenesis of F503Y, Y708D and K709I was conducted as described for V7 mutagenesis.

AAV vectors packaging

The rAAV vector backbone contains CBA (hybrid cytomegalovirus–chicken β-actin) promoter, woodchuck hepatitis virus posttranscriptional regulatory element (WPRE) and bovine growth hormone polyadenylation signal flanked by AAV2-inverted terminal repeats. Reporter gene—enhanced green fluorescent protein (referred as GFP) or therapeutic gene—human leptin cDNA and human adiponectin cDNA linked with a 2A sequence (referred as LEP/ADIPOQ) was cloned into polylinker sites of cis-plasmid as described previously.[7] LEP/ADIPOQ sequence was synthesized by gBlock of IDT. Plasmids used for viral packaging were prepared by using EndoFree plasmid Maxi and Mega Kit (Qiagen). Human embryonic kidney 293 cells were co-transfected with three plasmids—rAAV plasmid or cis-plasmid, AAV trans-plasmid encoding rep and cap genes including Rec2, Rec2.V1 to V8, AAV8, and AAV8 mutant, and adenoviral helper pF Δ6—using standard $CaPO_4$ transfection. AAV was purified from the cell lysate by ultracentrifugation through an iodixanol density gradient (OptiPrep Density Gradient Medium, D1556, Sigma). AAV was tittered using quantitative PCR using Step OnePlus Real-Time PCR System (Applied Biosystems) with the Power SYBR Green PCR Master Mix (Applied Biosystems#A25742).[47]

Administration of AAV vectors

AAV vectors were administered into mice either through i.p. injection in 150 μL AAV dilution buffer or via tail vein injection in 50 μL AAV dilution buffer. Doses ranging from 2E10 to 8E10 vg/mouse were used and specified in each experiment in figure legend.

GFP content measurement

GFP content was measured as previously described.[9] In brief, tissues were homogenized in ice-cold RIPA buffer (25mM Tris-HCl pH 7.6, 150mM NaCl, 1% NP-40, 1% sodium deoxycholate, 0.1% SDS) supplemented with proteinase inhibitors cocktail, followed by briefly sonication. The mixture was then spun at 13,000 rpm for 15 min at 4°C. The supernatant was collected. GFP fluorescence in 150 μL supernatant was measured with microreader (Synergy H1, Bio Tek Instrument) using a 485-nm excitation wavelength and cut-off 528-nm emission wavelength. GFP content was represented as readings after subtracting auto-fluorescence from GFP-null corresponding tissue and calibrated by either protein content in the samples or wet tissues weight.

ob/ob mice experiment

Male homozygous *ob/ob* mice (JAX 000632 B6.Cg-Lep^{ob}/J), seven weeks old, were randomly assigned to receive V7-GFP or V7-LEP/ADIPOQ. Sex and age-matched heterozygous *ob/+* mice received AAV buffer as another control. Body weight and food intake were monitored weekly over the period of 9 weeks. One mouse from V7-LEP/ADIPOQ 4E10 group and one mouse from V7-LEP/ADIPOQ 8E10 group were excluded due to technical errors of administration.

Glucose tolerance test (GTT)

Eight weeks after i.p. administration of AAV vectors, mice were i.p. injected with glucose solution (1mg glucose per gram body weight) after overnight fast with water *ad libitum*. Blood was collected from the tail at various time points and the blood glucose concentrations were measured with a portable glucose meter (Bayer Contour Next).

Rectal temperature measurement

Temperature probe (Physitemp, model BAT-12) topped with lubricant (white petroleum jelly) was used to measure the rectal temperature of *ob/ob* mice at 8-weeks after i.p. administration of AAV vectors.

Body composition by EchoMRI

EchoMRI was used to measure body composition of fat and lean masses in live mice without anesthesia at 9-weeks post AAV injection. EchoMRI imaging was performed with a 3-in-1 Analyzer (EchoMRI LLC, Houston, TX) according to manufacturer instructions at Small Animal Imaging Core of The Dorothy M. Davis Heart & Lung Research Institute, Ohio State University. Mice were subjected to a 5-Gauss magnetic

field and whole-body masses of fat, lean, free water, and total water were determined during separate cycles by manufacturer software comparison to a canola oil standard.

Serum harvest and analysis

Trunk blood was collected at euthanasia, clotted on ice, and centrifuged at 12,000 rpm for 15 min at 4°C. The serum was collected and stored at -20°C until further analysis. R&D Systems DuoSet ELISA kits were used to assay serum human leptin (R&D Systems, #DY398) and human adiponectin/Acrp30 (R&D Systems, # DY1065). Mouse serum insulin was measured with ELISA kit from ALPCO (ALPCO #80-INSMSU-E01). A Caymen Chemical colorimetric assay was used to determine serum glucose levels (#10009582).

Liver lipid extraction and triglycerides assay

Hepatic lipid was extracted from 50 mg of liver tissue from each animal by chloroform/methanol (2:1 v/v), followed by rinse in 50 mM NaCl and $CaCl_2$ (0.36M)/Methanol (1:1 v/v). An aliquot of the extract was mixed with Triton X100 and cold acetone, then was dried up and redissolved in PBS. Hepatic triglyceride quantification was performed with a Caymen Chemical triglyceride assay kit (Caymen Chemical, #10010303).

Immunoblotting

Tissues were homogenized in ice-cold Pierce RIPA buffer containing 1x Roche Phosstop and Calbiochem protease inhibitor cocktail III, then was subjected to brief sonication on ice. Tissues lysates were spun at 13,000 rpm for 15 min at 4°C. The supernatant was collected, and the protein concentration was assayed with BCA protein assay kit (Piece). 20 μg of protein from each sample was loaded and separated by gradient gel (4-20%, Mini-PROTEAN TGX, Bio-Rad), then transferred to a nitrocellulose membrane (BIO-RAD). Blots were incubated overnight at 4°C with the following primary antibodies, β-actin (Cell Signaling #4970, 1:1000), GFP (Santa Cruz Biotechnology, sc-9986 HRP, 1:1000). Chemiluminescence signal was detected and visualized by LI-COR Odyssey Fc imaging system (LI-COR Biotechnology, Lincoln, NE). Quantification analysis was carried out with image studio software version 5.2 (LI-COR Biotechnology).

Quantitative RT-PCR

Total RNA was isolated using the RNeasy Mini kit (QIAGEN) with RNase-free DNase treatment. cDNA was reverse transcribed using Taqman Reverse Transcription Reagents (Applied Biosystems). qPCR was carried out on StepOnePlus Real-Time PCR System using Power SYBR Green PCR Master Mix (Applied Biosystems). Primers were designed to detect GFP (GACTTCTTCAAGTCCGCCAT, TGTGGCTGTTGTAGTT GTACTC), ADIPOQ (AGGCAGGAAAGGAGAACCT, GTGGAGCCATCATAGTGGT), *Gapdh* (TCCCACTCTTCCACCTTCGA, TGCTGTAGC CGTATTCATTGTCA), and *Actinb* (ACCCGCGAGCACAGCTT, ATATCGTCATCCATGGCGAACT). Data were calibrated to *Actinb* and quantified using the $2^{-\Delta\Delta CT}$ method.

Viral vector copy number measurement

To assess vector biodistribution, viral vector copy number was measured as previously described.[9] Briefly, total DNA from various tissues was isolated using DNesay Blood and Tissue kit (Qiagen). GFP fragment was amplified and quantified by qPCR to determine the copy number of viral particle. 50 ng of DNA from each sample was used for real-time PCR with either duplicate or triplicate. Mouse nucleic genomic DNA fragment of GAPDH gene was used as control for mouse genetic DNA. Genomic DNA of untreated animals was also used as negative control for the comparison. Data are expressed as copies of V7-GFP/50 ng of genomic DNA.

QUANTIFICATION AND STATISTICAL ANALYSIS

Data are expressed as means ± SEM. GraphPad Prism 9 was used to analyze data. One-way ANOVAs with Tukey's *post hoc* test was utilized for comparisons between three or four groups. Time course data (BWs, GTT) were analyzed using a mixed ANOVA and area under the curve calculations were performed where applicable. Normality was tested using the Shapiro-Wilk method. * Indicates p value < 0.05; ** indicates p value < 0.01 in figures.